Plant, Cell & Environment

Plant, Cell and Environment (2016) **39**, 583–596 doi: 10.1111/pce.12657

Original Article

Drought limitations to leaf-level gas exchange: results from a model linking stomatal optimization and cohesion–tension theory

Kimberly A. Novick[1], Chelcy F. Miniat[2] & James M. Vose[3]

[1]*School of Public and Environmental Affairs, Indiana University, Bloomington, IN 47405, USA,* [2]*USDA Forest Service, Coweeta Hydrologic Laboratory, Otto, NC 28734, USA and* [3]*USDA Forest Service – Southern Research Station – Center for Integrated Forest Science. North Carolina State University, Department of Forestry and Environmental Resources, Raleigh, NC 27695-8008, USA*

ABSTRACT

We merge concepts from stomatal optimization theory and cohesion–tension theory to examine the dynamics of three mechanisms that are potentially limiting to leaf-level gas exchange in trees during drought: (1) a 'demand limitation' driven by an assumption of optimal stomatal functioning; (2) 'hydraulic limitation' of water movement from the roots to the leaves; and (3) 'non-stomatal' limitations imposed by declining leaf water status within the leaf. Model results suggest that species-specific 'economics' of stomatal behaviour may play an important role in differentiating species along the continuum of isohydric to anisohydric behaviour; specifically, we show that non-stomatal and demand limitations may reduce stomatal conductance and increase leaf water potential, promoting wide safety margins characteristic of isohydric species. We used model results to develop a diagnostic framework to identify the most likely limiting mechanism to stomatal functioning during drought and showed that many of those features were commonly observed in field observations of tree water use dynamics. Direct comparisons of modelled and measured stomatal conductance further indicated that non-stomatal and demand limitations reproduced observed patterns of tree water use well for an isohydric species but that a hydraulic limitation likely applies in the case of an anisohydric species.

Key-words: stomatal conductance; transpiration; isohydric; anisohydric; water use efficiency; capacitance.

INTRODUCTION

The stomatal conductance to CO_2 (g_c) is a critical determinant of plant response to drought (Oren *et al.* 1999; Sperry 2000; Flexas and Medrano 2002; McDowell *et al.* 2008) and directly influences photosynthetic assimilation (A), net primary productivity and mortality during periods of hydrologic stress (Leuning *et al.* 1995; Katul *et al.* 2000; McDowell *et al.* 2008; Katul *et al.* 2009; Medlyn *et al.* 2011). Achieving a mechanistic understanding of the dynamics of g_c during drought – a long-studied topic (Jarvis 1976; Cowan and Farquhar 1977; Hari *et al.* 1986; Tyree and Sperry 1988) – has become especially important in light of forecasts for more frequent and/or severe drought events in coming decades (Huntington 2006; Cook *et al.* 2015).

Herein, we consider a number of different mechanisms by which drought-related perturbations in water availability and vapour pressure deficit may affect g_c. Our study is focused in particular on the impacts of 'meteorological droughts' (Wilhite and Glantz 1985), which represent periods of precipitation deficiency, high temperatures and low humidity that can impact plant physiological functioning, even if they are relatively short in duration. The mechanisms that can limit g_c during meteorological drought include (1) supply, or hydraulic, limitations to plant water uptake imposed by progressively decreasing soil water potential; (2) 'demand limitations' to g_c imposed by excessively high vapour pressure deficit (hereafter D); and (3) non-stomatal limitations to a plant's photosynthetic machinery imposed by declines in leaf water status.

In the following introductory sections, we will review the biophysical underpinnings of these limiting mechanisms and will also discuss the potentially mitigating role of hydraulic capacitance during drought periods. The presentation of a model framework that considers the coordinated interaction of hydraulic, demand and non-stomatal limitations during drought forms the foundation of the rest of the manuscript. The work is motivated by the recognition that improving our understanding of drought effects on gas exchange across species is necessary to reduce uncertainty in earth system models (Dietze *et al.* 2014) and to develop the management practices that can ultimately limit tree mortality and other deleterious drought effects (Grant *et al.* 2013).

Hydraulic limitations to g_c

A growing body of literature (Meinzer *et al.* 2009; Choat *et al.* 2012; Martinez-Vilalta *et al.* 2014), grounded in cohesion–tension theory (van den Honert 1948; Tyree and Sperry 1988), highlights the important role of g_c in preventing the development of excessively negative water potentials in the leaf or the xylem that may promote catastrophic cavitation. Because some plants have been found to operate more closely

Correspondence: K. Novick. e-mail: knovick@indiana.edu

Published 2015. This article is a US Government work and is in the public domain in the USA.

to the point of hydraulic failure than others, plants are often classified along a continuum of leaf water potential regulation (Choat *et al.* 2012; Meinzer *et al.* 2014; Martinez-Vilalta *et al.* 2014). Plants that regulate g_c in such a way as to allow leaf water potential (hereafter Ψ_L) to approach the point at which excessive cavitation might occur are classified as more anisohydric. Examples of known anisohydric species include ring-porous *Quercus* species (Roman *et al.* 2015; Matheny *et al.* 2014) and *Juniper* species (Plaut *et al.* 2012; Meinzer *et al.* 2014). In contrast, isohydric plants regulate g_c to maintain a relatively stationary Ψ_L and a wide safety margin between the critical and actual water potentials (Choat *et al.* 2012; Sade *et al.* 2012; Klein *et al.* 2013) and include many *Pinus* species (Hacke *et al.* 2000; Plaut *et al.* 2012). The safety margin is often defined as the difference between midday water potential and the water potential at which a 50% loss in hydraulic conductivity occurs (Ψ_{50}, Choat *et al.* 2012). However, another work suggests that the difference between midday leaf water potential and the water potential at which air begins to enter the xylem (Ψ_e) may be a more appropriate way to define the safety margin, at least during well-watered conditions (Meinzer *et al.* 2009).

Demand limitations to g_c

Another body of work has focused on applying concepts from stomatal optimization theory (Cowan 1986; Cowan and Farquhar 1977; Berninger and Hari 1993) to develop closed-form models for the relationship between g_c and the atmospheric demand for water vapour (Buckley 2005; Katul *et al.* 2009; Katul *et al.* 2010; Manzoni *et al.* 2011; Medlyn *et al.* 2011; Vico *et al.* 2011; Palmroth *et al.* 2013; Buckley and Schymanski 2014). These studies rely on the assumption that stomata function principally to maximize carbon uptake for a given water loss over some finite time interval, which leads to declines in g_c with increasing D during dry periods when atmospheric demand for water vapour is high. Thus, in this work, we refer to limitations imposed by the optimization constraint as demand limitations.

A decline in g_c with increasing D is often observed (Oren *et al.* 1999) and is an important component of empirical and theoretical models for g_c (Jarvis 1976; Leuning *et al.* 1995; Katul *et al.* 2000). The direct physiological mechanisms responsible for the response of g_c to D have been the subject of much debate (Schulze *et al.* 1972; Franks *et al.* 1997; Comstock and Mencuccini 1998; Buckley 2005). For the purpose of this study, these mechanisms do not need to be formally specified; rather, the optimization theory simply requires that they have evolved to allow plants to achieve optimal stomatal functioning (Berninger and Hari 1993; Buckley 2005). While this approach has long been recognized as a useful way to conceptualize stomatal dynamics (Cowan and Farquhar 1977; Hari *et al.* 1986; Makela *et al.* 1996; Buckley 2005; Katul *et al.* 2009), with a few exceptions (e.g. Buckley 2005; Manzoni *et al.* 2013), the stomatal optimization approach has not been applied in a context that explicitly considers how hydraulic limitations to water supply in the leaf may also limit or co-limit gas exchange processes.

Non-stomatal limitations to g_c

Another research thrust has been focused on exploring how changes in leaf water status during periods of hydrologic stress affect gas exchange processes (Grassi and Magnani 2005; Niinemets *et al.* 2005; Lawlor and Tezara 2009) in ways that are independent, or at least quasi-independent, of stomatal limitations. These 'non-stomatal limitations' might include, for example, the generation of reactive oxygen species that damage ATP synthase (Tezara *et al.* 1999; Lawlor and Tezara 2009), other processes that limit the maximum carboxylation capacity of Rubisco (i.e. $V_{C,max}$) or diffusive limitations to the intercellular movement of CO_2 imposed by declines in mesophyll conductance (Grassi and Magnani 2005; Niinemets *et al.* 2009; Flexas *et al.* 2012). A notable feature of the model presented here is the capacity for these non-stomatal limitations to drive reductions in g_c, which is a feedback that has been proposed in other work (Buckley and Schymanski 2014).

The mitigating role of hydraulic capacitance

Finally, it is important to highlight recent advances in our understanding of how a reliance on stored water (or hydraulic capacitance) can mitigate limitations to g_c. It is increasingly recognized that plants may rely on the gradual depletion of stored water pools to support gas exchange processes at midday, when light and also vapour pressure deficit are high (Zweifel *et al.* 2001; Phillips *et al.* 2003; Scholz *et al.* 2011; Ward *et al.* 2013). Because hydraulic capacitance transiently decouples the flux of liquid water through the xylem from the transpiration flux, its role must be incorporated in any effort to link hydraulic and leaf-level limitations to gas exchange at sub-daily time steps.

A model framework that incorporates these concepts is developed and used here to address two principal research questions:

1. How do demand limitations, hydraulic limitations, non-stomatal limitations and hydraulic capacitance affect the dynamics of g_c during periods of hydrologic stress?
2. Can we detect and isolate these different limiting mechanisms in observed time series?

In developing the model, we draw on many previous studies that have already validated aspects of the hydraulic, demand and non-stomatal limitation mechanisms with observations (e.g. Berninger and Hari 1993; Grassi *et al.* 2009; Katul *et al.* 2010; Manzoni *et al.* 2011; Martinez-Vilalta *et al.* 2014). Here, we provide direct model-data comparisons for one isohydric and one anisohydric species and also explore the extent to which key model features are realized in observed time series of tree water uptake from a range of forest ecosystems in the Eastern USA. Our study is focused on general assessments of the model dynamics that we hope can motivate future hypothesis testing in empirical field studies or in studies that utilize publically accessible databases of plant physiological characteristics (e.g. the TRY database, Kattge *et al.* 2011).

MODELLING CONSIDERATIONS

As described in detail in the Supplementary Information (hereafter SI), the model development begins by linking Fick's law

of diffusion analogies for carbon assimilation (A) and transpiration (E) with a linear form of the Farquhar *et al.* (1980) model for photosynthesis. The model is not constrained by energy balance, which implies an infinite boundary layer conductance. The approach requires a third equation for g_c, which in this application comes from stomatal optimization theory. Models grounded in stomatal optimization theory begin with the assumption that stomata function explicitly to maximize the time and space integral of A for a given E. It follows that the resulting leaf carbon gain function

$$f = A - \mu E \tag{1}$$

reaches a local maximum when $df/dg_c = 0$. The parameter μ relates to the sensitivity of A to E (i.e. $\partial A/\partial E$), which is assumed constant over short (daily) time intervals (Manzoni *et al.* 2013; Buckley and Schymanski 2014). The constant value at which $\partial A/\partial E$ operates over a given day is noted as λ in some studies (Hari *et al.* 1986; Katul *et al.* 2009; Manzoni *et al.* 2011), although in other works, this same notation describes the variable's inverse (i.e. $\partial E/\partial A$, Cowan and Farquhar 1977). Here, we adopt the notation μ to avoid confusion. An increase μ may be interpreted as an increase in the time-integrated carbon cost of transpired water over the timescales at which μ is presumed to be constant.

As discussed in detail in the SI, if μ is known or assumed, a formulation for g_c may be achieved that does not require that the functional relationship between g_c and D be specified *a priori*. In the simple case of static leaf water potential (Ψ_L), the condition to maximize the function f is given as (Cowan and Farquhar 1977; Hari *et al.* 1986; Katul *et al.* 2009)

$$\frac{d[f(g_c)]}{d[g_c]} = \frac{\partial A}{\partial g_c} - \mu \frac{\partial E}{\partial g_c} = 0. \tag{2}$$

As described in Katul *et al.* (2010), and presented in the SI, computing the derivatives ($\partial A/\partial g_c$) and ($\partial E/\partial g_c$) produces the following expression for g_c for the case of static Ψ_L:

$$g_c = \left(\frac{a_1}{a_2 + sc_a}\right)\left[-1 + \left(\frac{c_a}{a\mu D}\right)^{1/2}\right] \text{(static}\Psi_L\text{)}. \tag{3}$$

Here, a_1 and a_2 are parameters relating to photosynthetic capacity, which depends on whether photosynthesis is light- or Rubisco-limited (e.g. $V_{C,max}$ and J_{max} in other literature, refer to SI for details), c_a is the atmospheric CO_2 concentration and a is the ratio of diffusivity of H_2O to CO_2 in air equal to 1.6.

In the more realistic scenario of dynamic Ψ_L at hourly to daily timescales, the dependency of A on Ψ_L and the sensitivity of Ψ_L to g_c must be considered. Specifically, the condition to maximize the function f, following Manzoni *et al.* (2011), becomes

$$\frac{d[f(g_c)]}{d[g_c]} = \frac{\partial A}{\partial g_c} + \frac{\partial A}{\partial \Psi_L}\frac{\partial \Psi_L}{\partial g_c} - \mu \frac{\partial E}{\partial g_c} = 0 \ \text{(dynamic } \Psi_L\text{)}. \tag{4}$$

The dependency of A on Ψ_L, which represents non-stomatal limitations to photosynthetic capacity, is expressed by relating a_1 to leaf water potential with an empirical function of the form

$$a_1 = a_{1,ww} \exp\left(b_1 |\Psi_L|^{b_2}\right), \tag{5}$$

after Vico & Porporato (2008), where $a_{1,ww}$ is the photosynthetic capacity under well-watered conditions and b_1 and b_2 are empirical constants. The relation between g_c and Ψ_L is developed by assuming that the transpiration rate, E, is equal to the sum of water flux through the stem (J_s) and the contribution of stored water to leaf water supply (F_S), giving $E = K(\Psi_s - \Psi_L) + F_S$ if gravitation head losses are neglected. This relation can be solved for Ψ_L, yielding

$$\Psi_L = \Psi_S - \frac{E - F_S}{K} = \Psi_S - \frac{\left(ag_c + g_{c,o}\right) f_1(T) D - F_S}{K} \tag{6}$$

where Ψ_S is soil matric potential, K is whole plant hydraulic conductance, $g_{c,o}$ is cuticular conductance to water vapour, F_S is the capacitive flux of stored water and $f_1(T)$ is a temperature-dependent constant that is necessary to include when D is expressed in units of kPa as opposed to a molar ratio.

The expression for g_c that follows from Eqns. 4 to 6 is unwieldy and thus is not presented here, although model closure for E, A, g_c and Ψ_L is achieved provided μ is specified; more details on the implementation of the modelling approach are presented in SI.

It has been previously proposed that μ may increase during periods of water limitation (Makela *et al.* 1996), and recent work has confirmed the expectation of an adaptive μ by showing that across a wide range of species, μ increases with decreasing leaf water potential in a generic way (Manzoni *et al.* 2011). Here, we incorporate this adaptability of μ by using a modified version of the relationship proposed by Manzoni *et al.* (2011):

$$\begin{aligned} \mu &= \mu_{WW} \exp\left(\beta_o\left[\Psi_{L,PREV} + \Psi_o\right]\right) && \text{for } \Psi_L < \Psi_o \\ \mu &= \mu_{WW} && \text{or } \Psi_L \geq \Psi_o \end{aligned} \tag{7}$$

where μ_{WW} is the marginal water use efficiency for well-watered conditions, β_o (which is negative) is a shape parameter and $\Psi_{L,PREV}$ is the average midday Ψ_L on the day preceding the simulation period. By linking μ to $\Psi_{L,PREV}$ as opposed to Ψ_L, we effectively permit μ to vary over daily as opposed to hourly timescales, consistent with the expectation that it is relatively constant over the course of a given day. This formulation assumes that there is some range of Ψ_L (i.e. $\Psi_o \leq \Psi_L \leq 0$) over which μ is insensitive to Ψ_L.

The optimality condition produces an atmospheric 'demand' limitation to stomatal conductance driven by increases in D even in the absence of changes in soil water potential, which is evident in the dependence of g_c on $D^{-1/2}$ in Eqn. 3. A 'hydraulic' limitation will apply when the Ψ_L necessary to support the demand-limited g_c is more negative than a prescribed critical minimum leaf water potential (Ψ_{CRIT}), below which rapid hydraulic failure may ensue. We note that it is not necessary to explicitly link Ψ_{CRIT} to either Ψ_e or Ψ_{50} for the purposes of exploring general model dynamics. When the Ψ_L necessary to support the optimal

g_c is less than Ψ_{CRIT}, the formulation for g_c is no longer derived from the optimization constraint; rather, the stomatal conductance is determined by inverting Eqn. 6 with $\Psi_L = \Psi_{CRIT}$.

To summarize, the model considers three potentially limiting mechanisms to g_c and other gas exchange variables during drought and one mitigating factor. The first is the *demand limitation* to g_c driven principally by D, which derives from the optimality assumption. The second is the *hydraulic limitation* imposed when the Ψ_L necessary to sustain optimal g_c is more negative than Ψ_{CRIT}; in this case, the formulation for g_c is determined from Eqn. 6. The third is *non-stomatal limitation* to gas exchange, driven by the decrease in a_1 with increasing Ψ_L (Eqn. 6) and/or the increase in μ with Ψ_L (Eqn. 7). In addition, via the inclusion of a stored water flux term (i.e. F_s in Eqn. 6), the model also accommodates the important role that *hydraulic capacitance* may play in mitigating any of these three limitations to gas exchange during periods of hydrologic stress.

METHODS

Generalized model simulations – driving variables, parameterization and analysis

All model simulations were driven by observations of D, photosynthetically active radiation (Q), air temperature and soil water potential (Ψ_s) that were observed within a 20-year-old loblolly pine forest near Durham, North Carolina from August 24 to September 12, 2005 (refer to SI and Stoy *et al.* 2006; Novick *et al.* 2014). During this time period, only 2 mm of precipitation fell on the site, promoting mild meteorological drought conditions characterized by increasing D and steadily decreasing Ψ_s (refer to supplementary Fig. S1).

The model was run for a range of scenarios reflecting various assumptions about the limiting mechanisms to leaf gas exchange and the role of stored stem water. First, the model was run for the simple case of no hydraulic constraint, no capacitance and no sensitivity of μ or a_1 to Ψ_L (case 1, Table 1). In case 2, a hydraulic constraint is imposed by requiring $\Psi_{CRIT} > -1.8$ MPa, which is an arbitrary value selected to be higher than the lowest values of midday Ψ_L observed for the case 1 simulations. In case 3, the parameter μ varies with Ψ_L accordingly, with a sensitivity $\beta_o = -1.5$. In case 4, the parameter a_1 varies with Ψ_L, with a sensitivity $b_1 = -0.5$. Finally, case 5 is identical to case 2, but with an assumed contribution of stored water flux to E. The F_S flux was assumed to be positive during the morning (representing depletion of stored water) and negative in the afternoon and evening (representing xylem refilling, refer to SI for more details), consistent with previously published F_s data from a range of biomes (Phillips *et al.* 2003; Meinzer *et al.* 2004).

We focused our analysis of model outputs on the relationships between E, g_c and D over the course of the dry-down event. Of particular interest is the extent to which the relationship between g_c and D varies in time. In the case where the demand limitation is the only limitation to gas exchange, the relationship between these two variables takes the form

$$g_c = b + mD^{-1/2}, \tag{8}$$

where the slope and intercept parameters may be predicted directly from the value of c_a, a_1, a_2 and μ (refer to Eqn. 3). When μ changes over the course of the dry-down event (reflecting non-stomatal limitations), or in the presence of a hydraulic limitation or hydraulic capacitance, the mathematical framework of the model does not permit elegant, analytical representations for the slope and intercept parameters. Thus, in this case, the parameters b and m were determined by directly linear regression of the modelled g_c as a function of $D^{-1/2}$.

Exploring the extent to which model features are observed in empirical data

After summarizing the distinguishing features of each limiting mechanism to gas exchange, we explored the extent to which these features were observed in field observations of tree water use. In mixed canopies and in the absence of time-intensive measurements of leaf gas exchange, a convenient proxy for E is xylem sap flux measurements (Oren *et al.* 1999). Thus, our application of the model framework focuses on the dynamics of the 'apparent' rates of transpiration and stomatal conductance observed in field sap flux data, hereafter E_{SF} and $g_{c,SF}$, where the subscript 'SF' stands for sap flux. Practically, E_{SF} is a proxy for $K(\Psi_S - \Psi_L)$, and $g_{c,SF}$ is thus

Table 1. The characteristics of the various model scenarios

	Sensitivity of μ to Ψ_L	Sensitivity of a_1 to Ψ_L	Hydraulic constraint	Capacitance?
Case 1 (demand limitation only)	None	None	None	No
Case 2 (demand limitation + hydraulic limitation)	None	None	$\Psi_{CRIT} = -1.8$ MPA	No
Case 3 (demand limitation + non-stomatal limitation via μ)	$\beta_o = -1.5$	None	None	No
Case 4 (demand limitation + non-stomatal limitation via $V_{c,max}$)	None	$b_1 = -0.5$	None	No
Case 5 (identical to case 2 but with a prescribed capacitive flux	None	None	$\Psi_{CRIT} = -1.8$ MPA	Yes

Other model parameters are specified in the SI.

$$g_{c,SF} = \frac{E_{SF}}{Df_1(T)} = \frac{K(\Psi_S - \Psi_L)}{Df_1(T)} - g_{c,o}. \quad (9)$$

In the event of little to no reliance on stored water and non-limiting boundary layer conductance, E will be closely coupled to E_{SF} and g_c will be closely coupled to $g_{c,SF}$. Otherwise, predictive relationships determined for E and g_c may not apply to the proxies derived from sap flux data.

Xylem sap flux and relevant meteorological variables were monitored continuously from 2010 to 2012 in six Eastern US forest ecosystems as part of the USDA Forest Service Remote Assessment of Forest Ecosystem Stress (RAFES) project. Details on the sap flux methodology are presented in the SI. In each study site, we identified a period of 2–3 months during the growing season that included a significant dry-down period of at least 10 days and was associated with a clearly observable decline in soil moisture content. Data were then classified on the basis of soil moisture into relatively wet, intermediate or dry periods. The diurnal patterns of sap flux, the ratio of nocturnal to daytime sap flow and the slope and intercept of the function $g_{c,SF} = b + mD^{-1/2}$ were determined in each site period (refer to SI for details).

Species-specific model simulations for comparison with observations

To evaluate the ability of the model to reproduce observed gas exchange dynamics directly, we produced additional model simulations for two species (*Pinus taeda* and *Quercus alba*) growing in the Duke Upper RAFES site. We selected these species for two reasons. First, they span a gradient of isohydric to anisohydric behaviour. *P. taeda*, like many conifers, is known to be very isohydric (Hacke *et al.* 2000), whereas *Q. alba* is known to be more anisohydric (Roman *et al.* 2015). Second, the Duke Forest is an intensely studied ecosystem from which rich eco-physiological datasets have been produced (e.g. Hacke *et al.* 2000; Maherali *et al.* 2006; Domec *et al.* 2010), facilitating site- and species-specific model parameterizations. Details on the parameterization approach are given in the SI. The biggest difference between the two parameterizations was introduced through the formulation for K. Using hydraulic vulnerability curves previously reported by Maherali *et al.* (2006), K was prescribed to be relatively low and insensitive to Ψ_L for the isohydric *P. taeda* and relatively high and highly sensitive to Ψ_L for the anisohydric *Q. alba*.

RESULTS

The effect of the various limitations on the dynamics of g_c, E and Ψ_L

In all model simulations, the daytime g_c decreased as the dry down progressed (Fig. 1a–c), reflecting demand limitation as D increased. When the optimization constraint is the only limitation to gas exchange (i.e. case 1), the decline in daytime g_c did not translate into a decline in daytime E (Fig. 1d–f, black lines) because a higher D will drive E forward even as it reduces g_c (refer to Eqn. S2 of the SI). A hydraulic limitation to gas exchange reduced the magnitude of daytime g_c and E relative to case 1 (black dashed line in Fig. 1a–f). When hydraulic limitations apply, they may be distinguished by the relatively constant E during the course of the day, over which timescales Ψ_S does not change considerably (Fig. 1e,f). Non-stomatal limitations to gas exchange, imposed either through increasing μ or decreasing a_1, also reduced the magnitude of both g_c and E relative to case 1 (gray lines in Fig. 1a–f). These reductions reflect the fact that metabolic limitations to photosynthetic functioning feedback into declines in g_c via the optimization constraint.

An important consequence of reductions to g_c imposed by non-stomatal or hydraulic limitations is an increase in the Ψ_L necessary to support the optimized gas exchange (Fig. 1g–h). In fact, for the scenarios presented in Fig. 1, minimum midday Ψ_L near the end of the dry-down period was similar to that at the start of the dry-down period (−1.5 to −1.8 MPa) regardless of whether hydraulic or non-stomatal limitations were applied, even though no explicit hydraulic constraint was imposed in the latter case. In the absence of either a non-stomatal or hydraulic limitation, the Ψ_L necessary to support the optimized gas exchange becomes excessively low near the end of the dry-down event (<−6 MPa, Fig. 1i), with large associated declines in K (Fig. 1l).

The relationship between g_c and D for the various model scenarios

When the optimization constraint is the only limitation to gas exchange, the slope of the relation between g_c and D (i.e. m) during conditions of non-limiting light is stationary over the course of the drought event (Fig. 2a). Non-stomatal limitations tend to decrease both g_c and the magnitude of m monotonically over the course of the dry-down event (Fig. 2e–h). This is true regardless of the mechanism by which they are imposed (i.e. variable μ or variable a_1), although the rate of change of m depends on the sensitivity parameters b_1 and β_o (Fig. 3a,b, respectively). The effect of hydraulic limitation on the relationship between g_c and D depends on the value of Ψ_{CRIT}. When Ψ_{CRIT} is relatively low, the slope parameter m increases over the course of the dry-down event (Figs. 2d & 3c). However, for higher Ψ_{CRIT}, the slope parameter m may decrease in time as the difference between Ψ_{CRIT} and Ψ_S becomes smaller. In the extreme case where $\Psi_{CRIT} > \Psi_S$, gas exchange no longer proceeds, and the slope parameter m is driven to zero (Fig. 3c).

An interesting feature of the model simulations is that the hysteresis in the relationship between hourly E and D, when visualized over the course of a single day, tends to increase as the dry-down progresses (Fig. 4a–c). This feature is most pronounced when the optimization constraint is the only mechanism limiting gas exchange (Fig. 4a–c, black lines) and is driven by a phase lag between radiation (which peaks around noon) and D (which peaks several hours later). Another interesting feature of the demand limitation is the capacity for E to peak at some intermediate D provided μ is sufficiently high (Fig. 4d).

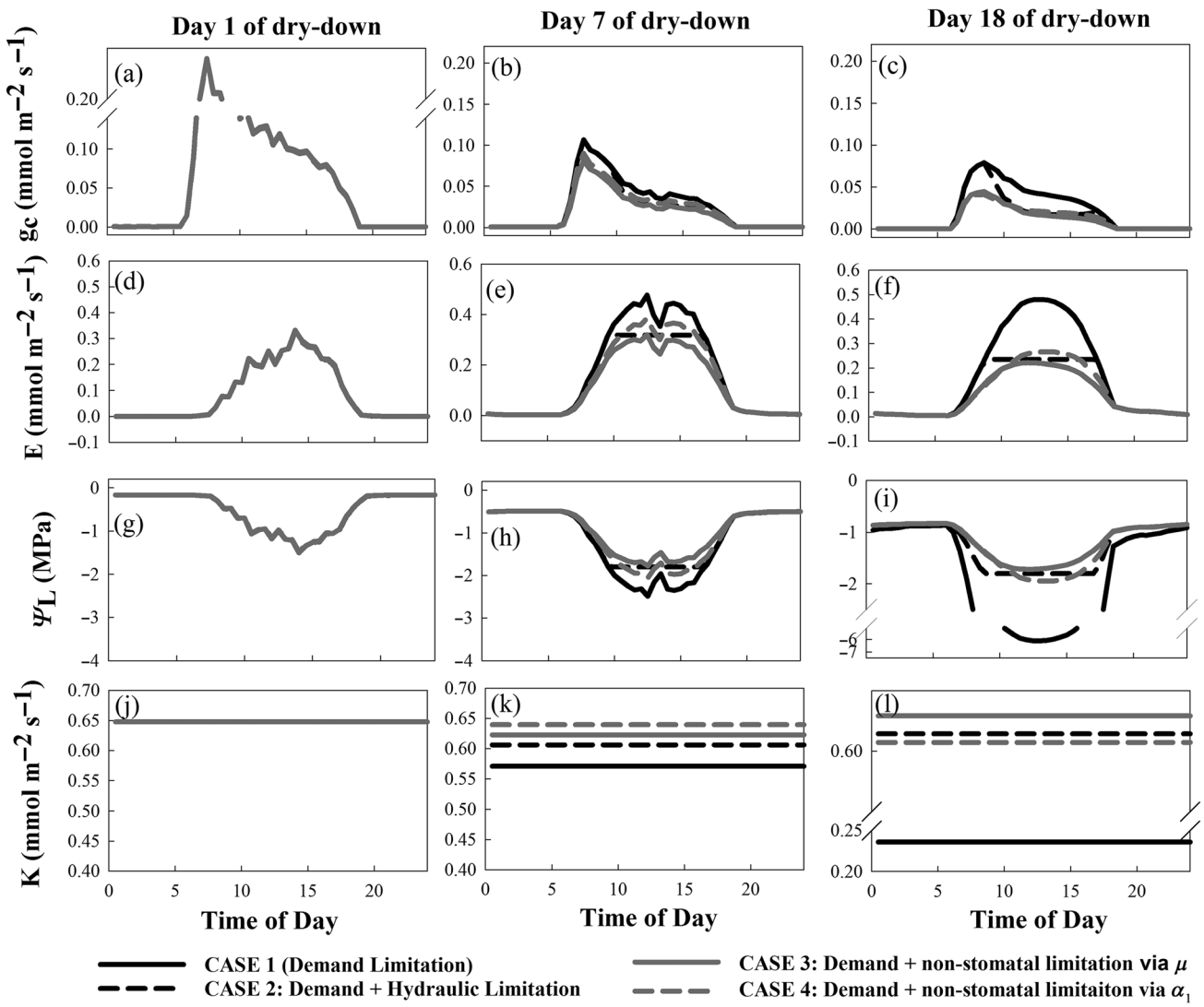

Figure 1. The daily time course of key model variables for various stages of the dry-down event. The top row shows the stomatal conductance to CO_2 (g_c), the second row shows the leaf-specific transpiration rate (E), the third row shows the leaf water potential (Ψ_L), and the fourth row shows the leaf-specific hydraulic conductivity (K). The legend is given at the bottom of the figure. Early in the dry-down, the daily time course of all four model cases is identical (thus, only one line is visible).

Mediating influence of stored water under hydraulic limitation

A defining characteristic of a reliance on stored water is a decoupling between E and the stem water flux (e.g. E_{SF}), with the contribution of the stored water flux to E_{SF} being relatively low during daytime periods and relatively high during afternoon and nocturnal periods (Fig. 5a–b). The dynamics of leaf-level g_c and the stomatal conductance that can be inferred from stem sap flux (e.g. $g_{c,SF}$) are also decoupled in the case of a strong reliance on stored water, with E_{SF} and $g_{c,SF}$ underestimating the true E and g_c in the morning and overestimating them in the afternoon (Fig. 5a,b). Additionally, as illustrated in Fig. 5a, the F_s assumed in these simulations requires some evening refilling of depleted water stores, leading to relatively high E_{SF} during the hours between sunset and midnight.

The defining features of the limiting mechanisms to gas exchange and their links to field observations

The defining characteristics of demand, hydraulic and non-stomatal limitations are summarized in Table 2. It is important to note that these features apply to the case of little to no reliance on stored water. If hydraulic capacitance is large, then transpiration inferred from stem sap flux (e.g. E_{SF}) and E become decoupled (as do g_c and $g_{c,SF}$, Fig. 5). The occurrence of nocturnal stem water movement in order to refill stored water pools and embolized xylem elements may be an important indicator of a reliance on hydraulic capacitance (Fig. 5a).

Many of the distinguishing features of each limitation scenario were realized in the sap flux observations, as detailed in Table 3. Even during relatively well-watered conditions, the $g_{c,SF}$ decreased significantly with increasing D according

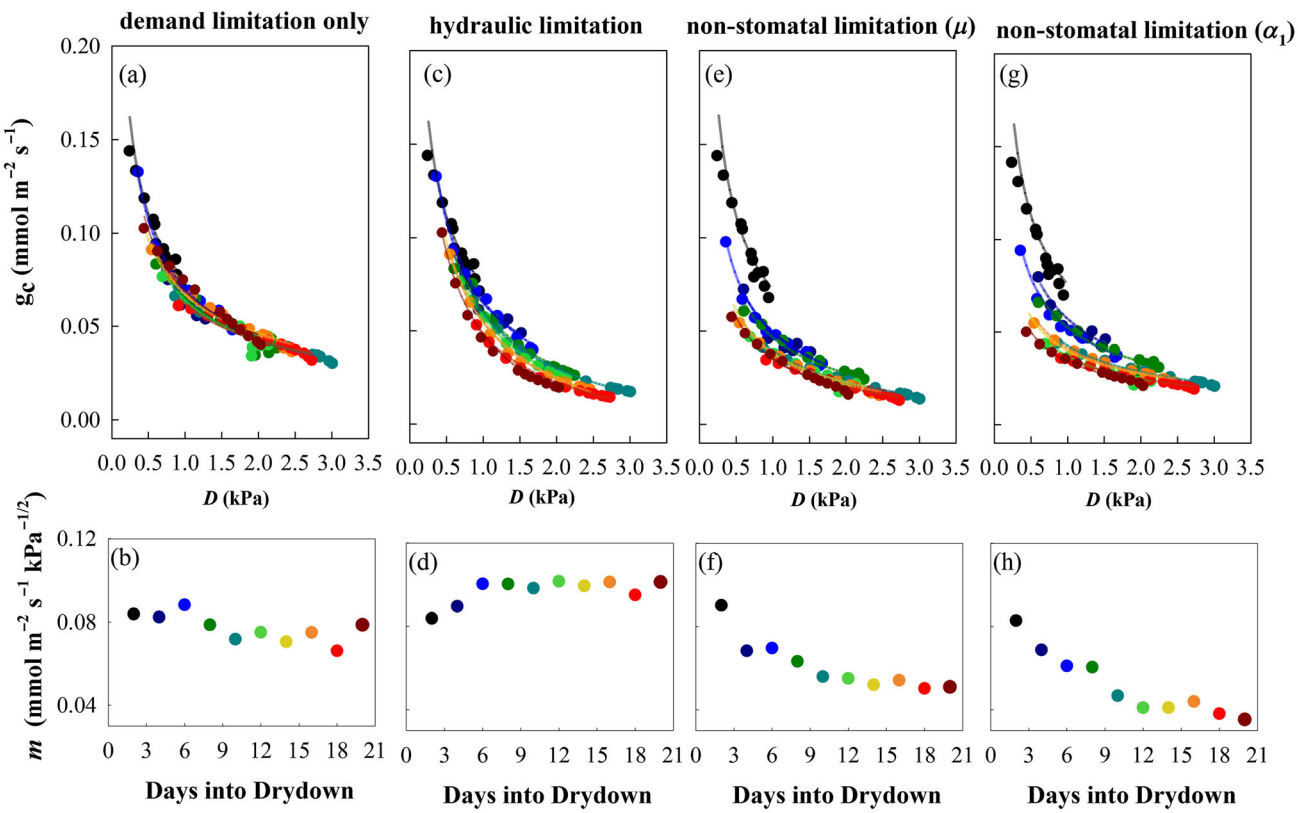

Figure 2. The dynamics of the relationship between between $g_{C,SF}$ and D over the course of the dry-down period depends on the limiting mechanism. The top row of panels shows this relationship for nine representative days of the dry-down period for conditions of non-limiting light. The bottom row of panels shows the temporal trends in the slope parameter (m) of the relationship $b + mD^{-1/2}$ (i.e. Eqn. 8) over the same 9 days. The colours in the top panels correspond to the day of the dry-down period (refer to x-axis of bottom panels).

to $g_{c,SF} = b + mD^{-1/2}$ for nearly every site species, which is an evidence of the demand limitation. A trend of increasing clockwise hysteresis in the diurnal relationships between E and g_c, another hallmark of the demand limitation, was observed in 7 of the 12 site species (Table 3). A graphical presentation of these dynamics is included as SI Fig. S3.

Stationary midday E_{SF}, which may be indicative of a hydraulic limitation, was observed for four of the site species combinations: *Liriodendron tulipifera* and *P. taeda* in the Duke Lower site, *Pinus palustris* in the Jones Center site and *P. taeda* in the Crossett EF site, noting that the latter two sites are the most xeric sites in the network. In a number of other sites, the relationship between E_{SF} and D was peaked, with a clear maximum E_{SF} occurring at an intermediate D. Such a feature may evolve from the demand constraint (Katul *et al.* 2010; Manzoni *et al.* 2011) if μ is sufficiently high (Fig. 4d).

The slope parameter m decreased as conditions progressed from wet to dry in most site species, which is indicative of non-stomatal limitation in the absence of stations midday E_{SF}. In the Jones Center's *P. palustris* and in the Crossett EF site's *P. taeda* trees, the ratio of nocturnal:total E_{SF} increased significantly over the course of the dry-down event, to a ratio of 0.21 in the former and 0.34 in the latter. Thus, in these sites, a reliance on hydraulic capacitance may alleviate the hydraulic or non-stomatal limitations to gas exchange processes.

Evaluating the model's ability to reproduce observed water use dynamics for an isohydric and anisohydric species

The results presented in Table 3 show that many of the features of the model are realized in the observed time series. For a more formal test of the functionality of the model, we compare measured and modellsed g_c for two species growing in the Duke Upper site: the isohydric *P. taeda* and anisohydric *Q. alba*. We focus our evaluation on daily averaged midday g_c during periods of high-light conditions, when boundary layer conductance is likely to be high (consistent with model assumptions). The conductance data were normalized by their well-watered values to obviate the need to scale the leaf-level model results to match the tree-level sap flux data. Finally, because the results of non-stomatal limitations on gas exchange are qualitatively similar regardless of whether they are imposed by variable μ or a_1 (i.e. Figs. 2 & 3), this comparison is simplified by considering only non-stomatal limitations imposed by variable μ.

For *P. taeda*, the model reproduced well the change in normalized midday g_c (Fig. 6a). Regardless of the choice of β_o, the correlation coefficient exceeds 0.80, and the mean absolute error was less than 10%. However, the lowest bias error was associated with an intermediate sensitivity of μ to Ψ_L ($\beta_o = -0.56$, filled circles in Fig. 6a). It is important to note that

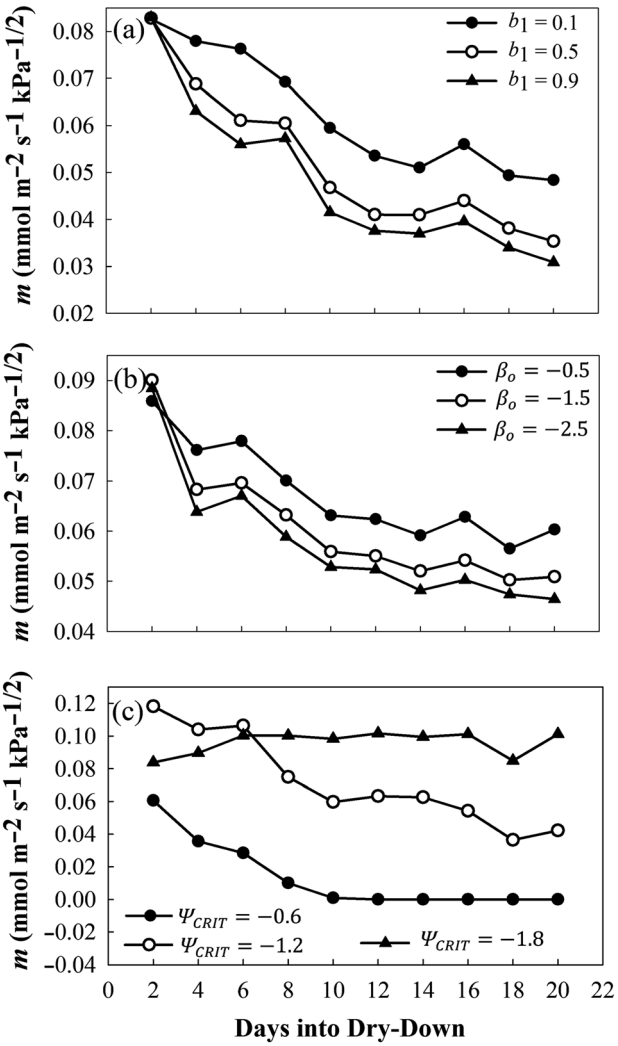

Figure 3. The change in the stomatal sensitivity parameter m depends on the sensitivity of α_1 to Ψ_L (e.g. b_1, a), on the sensitivity of μ to Ψ_L (e.g. β_o, b) and on the critically limiting value of Ψ_L in the case of a hydraulic limitation (i.e. Ψ_{CRIT}, c). In the simulations of (a) and (b), no hydraulic limitation applies. In the simulations of (c), both b_1 and β_o are held constant.

the results shown in Fig. 6a represent simulations for which a hydraulic constraint does not apply; rather, the reductions in g_c are driven by increasing D over the course of the dry-down event, with additional reductions in g_c promoted by the non-stomatal limitation imposed by a non-zero β_o. Relatedly, provided $\beta_o > 0$, the modelled Ψ_L is maintained to be at or above −2.0 MPa (Fig. 6b). For *P. taeda* trees growing in this site, measured Ψ_e and Ψ_{50} were −2.0 and −3.1 MPa, respectively (Maherali *et al.* 2006). Thus, when non-stomatal limitations apply, the model predicts a positive safety margin, regardless of how it is defined, without any reliance on a direct hydraulic limitation (although it should be noted that the parameters Ψ_e and Ψ_{50} are not necessarily static in time, Lens *et al.* 2011).

For *Q. alba*, results were more mixed. The correlation coefficient was lower ($r^2 = 0.61$–0.71), and the mean absolute error was higher (12–17%) for the simulations illustrated in Fig. 6c. These scenarios represent a non-stomatal limitation with a high β_o (1.5) and non-stomatal + hydraulic limitations with $\Psi_{CRIT} = -0.55$ or −1.1 MPa. We note that −0.55 and −1.1 MPa are representative of the Ψ_e and Ψ_{50}, respectively, previously determined for this site species (Maherali *et al.* 2006). When no hydraulic limitation applies (triangles in Fig. 6c), the modelled g_c is driven to zero late in the drawdown by hydraulic failure (i.e. Ψ_L becomes excessively low and K is driven to zero). When the $\Psi_{CRIT} = -0.55$ MPa (crosses in Fig. 6c), the modelled g_c is also driven to zero late in the drawdown when the Ψ_S becomes more negative than Ψ_{CRIT}. When $\Psi_{CRIT} = -1.1$ MPa and $\beta_o = 1.5$ (circles in Fig. 6c), the modelled g_c remains positive throughout the simulation period but is nonetheless underestimated late in the drawdown when the measured $g_{c,SF}$ is low. This model-data mismatch could be explained by capacitance, which is implied by the fact that the ratio of nocturnal:total daily E_{SF} increased for this species late in the dry-down period (Table 3). It could also be explained by the fact that *Q. alba* trees tend to have deep roots, which would increase the integrated Ψ_S over the rooting depth (Roman *et al.* 2015). Finally, the underestimation could be linked to an imperfect parameterization scheme that could be improved with additional benchmarking. For the purposes of this particular study, however, the most relevant result is that a hydraulic limitation likely applies for this site species.

DISCUSSION

The model framework presented here was designed to explore how the dynamics of gas exchange rates are limited or co-limited by demand limitations linked to optimal stomatal functioning, hydraulic constraints and non-stomatal limitations to leaf physiological functioning. We used the model outputs to illustrate that gas exchange dynamics for each limitation are associated with unique dynamical characteristics (Table 3) and confirmed that these features are often realized in empirical field observations of tree water use dynamics (i.e. Table 3, Fig. 6). A direct model-data comparison also confirmed the functionality of the model (i.e. Fig. 6).

We showed, using both model outputs and empirical observations, that demand and non-stomatal limitations to gas exchange can sufficiently reduce the demand for water in the leaf such that direct hydraulic limitations can often be avoided (i.e. Figs. 1 & 6). Specifically, there is a tendency for g_c to decrease rapidly with increasing D when μ increased, or a_1 decreased, with declining leaf water status (Fig. 2). As a result, excessive declines in Ψ_L are avoided, promoting larger hydraulic safety margins. When viewed in light of recent synthesis studies showing that, when compared with angiosperms, gymnosperms tend to have higher μ (Manzoni *et al.* 2011) and also higher safety margins (Choat *et al.* 2012; Johnson *et al.* 2012), the results from the present study highlight that species-specific 'economics' of stomatal behaviour (as represented by the magnitude of μ) may play an important role in differentiating species along the continuum of isohydric to anisohydric behaviour. This implication will be discussed in more detail in the

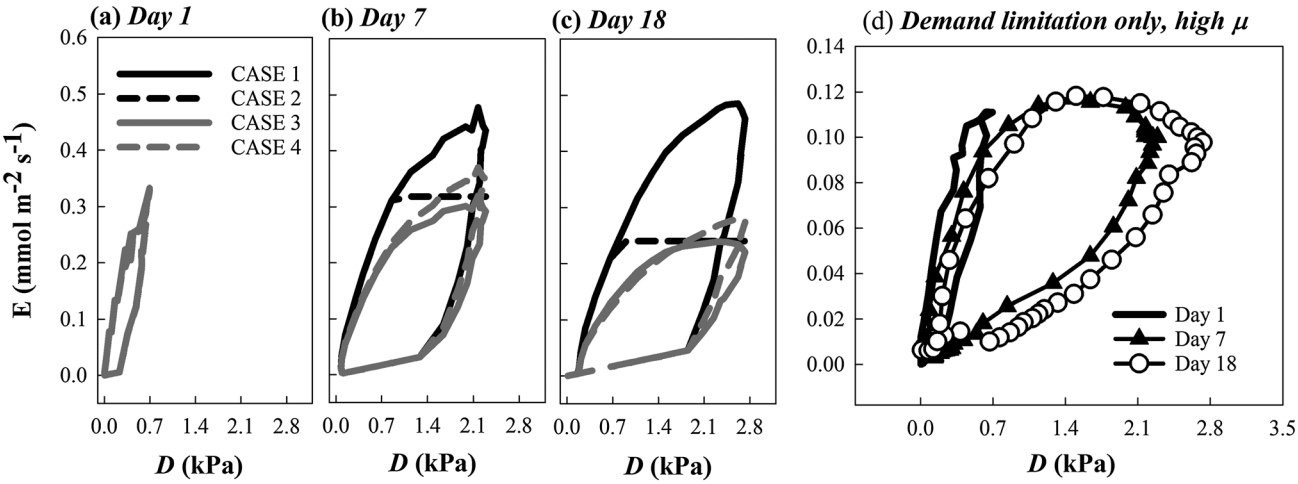

Figure 4. The trajectory of hourly leaf-specific transpiration (E) as a function of D during different stages of the dry down (a–c). When the demand limitation imposed by the optimization constraint is the only limiting mechanism to gas exchange (black lines), increasing clockwise hysteresis as the drought progresses is observed. Both non-stomatal (gray lines) and hydraulic limitations (black dashed lines) tend to reduce the extent of the hysteresis and the magnitude of the gas exchange variables. The direction of the hysteresis, which is the same in all panels, is indicated in (b). Panel (d) shows that when the parameter μ is high (in this case 80 μmol mol^{-1} kPa^{-1}), the demand limitation produces a peak in daytime E at intermediate D. The value of μ associated with the case 1 simulations shown in (a)–(c) was 21 μmol mol^{-1} kPa^{-1}.

succeeding texts, following a brief discussion on some of the features of the demand limitation to gas exchange imposed by the optimization constraint.

Some notable characteristics of the demand limitation

The demand limitation to g_c is driven by the assumption that stomatal behaviour has evolved to achieve the goal of maximizing carbon uptake while minimizing water loss, which requires a decrease in g_c with increasing D (Katul *et al.* 2009; Figs. 1, 2). An important characteristic of the optimization constraint is a strong relationship between g_c and $D^{-1/2}$ (Fig. 2); in the absence of non-stomatal or hydraulic limitations to gas exchange, the parameters of this relationship do not change as drought progresses (i.e. Fig. 2a). A significant relationship between g_c and $D^{-1/2}$ was detected in most of the empirical time series (Table 3). Furthermore, previous work has shown that the relationship between g_c and $D^{-1/2}$ that evolves from the optimization constraint is consistent with a wealth of previously published results (Oren *et al.* 1999; Katul *et al.* 2009).

When the full diurnal range of light conditions is considered, the demand constraint produces pronounced clockwise hysteresis in the relationship between gas exchange variables and D (Figs. 2 & 3), which increases as a dry-down event progresses in the absence of significant non-stomatal or hydraulic limitation (Figs. 2 & 3). Similar clockwise hysteresis has been observed in other studies (Wullschleger *et al.* 1998; O'Grady *et al.* 1999; Ford *et al.* 2004; Ewers *et al.* 2005; Zhang *et al.* 2014), although again, the mechanism promoting this hysteresis is not clear (O'Grady *et al.* 1999; Unsworth *et al.* 2004; Zhang *et al.* 2014). Our results suggest that the principle driver of this hysteresis is the phase lag between light (i.e. Q) and D, confirming results from Zhang *et al.* (2014) and Ford *et al.* (2005). Finally, we note that the demand limitation can also promote the occurrence of a maximum E at some intermediate value of D (Fig. 5d), which cannot be produced by hydraulic limitations alone unless K declines rapidly over the course of a given day. A peaked relationship between E_{SF} and D was observed in many of the empirical time series (Table 3).

The relationship between the degree of isohydry and the limiting mechanisms to gas exchange

Our study is novel in that our model proposes that non-stomatal limitations to gas exchange feedback through the optimization constraint to reduce g_c and increase Ψ_L (Fig. 2) and thus may be an important determinant of a plant's positioning along the isohydric–anisohydric spectrum. In support of this proposition, we show that characteristics of a demand and non-stomatal limitations to gas exchange (i.e. significant relationship between g_c and $D^{-1/2}$, increasing hysteresis in the relationship between E and D, decreasing m under dryer conditions) were realized in empirical observations of tree water use from a range of species growing in a range of Eastern US biomes (Table 3).

We also demonstrated, through a species-specific calibration of the model, that demand and non-stomatal limitations to gas exchange together explained well the dynamics of stomatal conductance observed for *P. taeda*, which is an isohydric species (Fig. 6a). In particular, these limitations promoted relatively stationary midday Ψ_L (Fig. 6b) that remained greater or higher than both the Ψ_e and Ψ_{50} previously reported for this site species (Maherali *et al.* 2006). In the case of the more anisohydric *Q. alba*, we showed that a hydraulic constraint was necessary, in addition to non-stomatal and demand limitations, to prevent Ψ_L from dropping below the species-specific $\Psi_{L,50}$, at which point the model predicts that hydraulic failure rapidly ensues (Fig. 6c–d). Even when a hydraulic constraint is applied, the

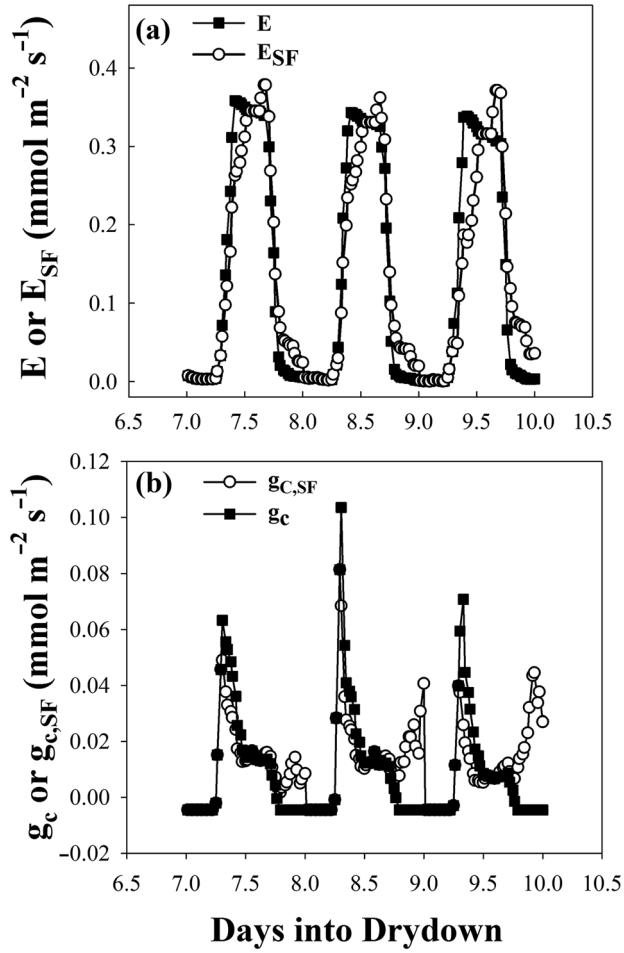

Figure 5. A reliance on stored water decouples the dynamics of E and E_{SF} (a) and g_c and $g_{c,SF}$ (b).

model still underestimates the stomatal conductance during the driest periods. This underestimation may be linked to hydraulic capacitance and species-specific differences in rooting depth or may reflect an imperfect parameterization scheme that could be improved upon with further model benchmarking.

The literature provides ample support for the notion that non-stomatal constraints, including reductions in photosynthetic capacity (i.e. V_{cmax}) and mesophyll conductance, are important controls on plant gas exchange during drought. For example, many studies report that V_{cmax} declines with declining soil water potential, often by orders of magnitude (Flexas *et al.* 2002; Limousin *et al.* 2010; Zhou *et al.* 2014) and that these limitations combined can explain 30–50% of the observed declines in photosynthesis during drought periods (Limousin *et al.* 2010; Zhou *et al.* 2014). To our knowledge, no previously published study reports on the time evolution of $V_{c,max}$, g_c, Ψ_L and the hydraulic safety margin during drought for multiple species spanning a gradient of isohydric and anisohydric behaviour. Such a dataset is certainly motivated by this study, as it would present a unique opportunity for a more rigorous evaluation of model predictions. Nonetheless, previous work reporting on a direct relationship between mesophyll conductance and g_c, both within and across species (Limousin *et al.* 2010; Flexas *et al.* 2012; Niinemets *et al.* 2005; Loreto *et al.* 1992), provides some empirical evidence that a feedback between mesophyll conductance and g_c driven by the optimization constraint is possible, even if those relationships are insufficient to confirm the existence of this process directly.

Utility and limitations of the model and diagnostic framework

In developing the model, we strove to find a balance between analytical tractability and physical realism, which necessitated the inclusions of a number of simplifying assumptions into the model framework. First, our model is based on a linearized variant of the Farquhar *et al.* (1980) photosynthesis model, which may bias the model if it is applied to conditions characterized by high c_a (Katul *et al.* 2010). Second, in order to maintain analytical tractability, the model also neglects the effect of dynamic temperature on optimal gas exchange, although recent work suggests that those dynamics may be important (Duursma *et al.* 2014). Finally, our model also assumes that boundary layer conductance is never limiting, which may be a reasonable assumption during most daytime periods (Kim *et al.* 2014) but may not be a good assumption during early morning or when humidity is high. Our formulation of the stored water flux is rather coarse and requires that it be specified; future developments could focus on more directly integrating the role of capacitance in the optimization framework. We also note that modelled processes discussed here are representative of a rather specific combination of physiological capacity

Table 2. The salient identifying characteristics of demand, hydraulic and non-stomatal limitations to gas exchange, which may inform the diagnosis of limiting mechanisms in field observations

Feature	Demand limitation	Hydraulic limitation	Non-stomatal limitations
Hysteresis between E and D at hourly timescales	Increases as drought progresses	Reduced compared with the case of demand limitation alone	Reduced compared with the case of demand limitation alone
Hysteresis between midday g_c and D at daily timescales	None	Pronounced	Pronounced
Relationship between g_c and $D^{-1/2}$	Does not change as drought progresses	The slope parameter m may increase or decrease	The slope parameter m decreases over the course of the drought
Other features	Potential for E to peak at some intermediate D	Stationary E and Ψ_L during midday	Promotes less negative Ψ_L during periods of hydrologic stress

Table 3. Characteristics of the study sites and features of the observed dynamics of stem water flow (E_{SF}) and the apparent stomatal conductance derivable from E_{SF} (i.e. $g_{c,SF}$, refer to Eqn. 9) for relatively dry, intermediate (Int) and wet conditions

Site	Lat (N) Lon (W)	Species	m (r^2)			Δm		Ratio of nocturnal to total daily E_{SF}			Patterns in daytime E			Hyst?	Governing mechanism
			Wet	Int	Dry	Dry-wet	Int-wet	Wet	Int	Dry	Wet	Int	Dry		
Coweeta	33.05 83.42	*Quercus alba*	8 (.48)	5 (.18)	6 (.38)	[a]	[a]	.12	.11	.01	MI	MI	MI	NC	D, non-S
		Acer rubrum	2 (0.9)	ns	ns	ns	ns	.16	.12	.15	MI	MI	MI	NC	
		Liriodendron tulipifera	3 (.43)	1 (.29)	ns	[a]	ns	.17	.11	.15	MI	MI	MI	NC	DL
Duke Lower	33.9879.09	*Acer rubrum*	28 (.93)	22 (.91)	22 (.91)	[a]	[a]	.08	.07	.09	PK	PK	PK	I	D, non-S
		Pinus taeda	10 (.63)	6 (.63)	6 (.50)	[a]	[a]	.12	.09	.09	MI	ST	PK	I	D, H, non-S
		Liriodendron tulipfera	12 (.71)	10 (.86)	9 (.86)	[a]	[a]	.09	.07	.09	MI	ST	ST	I	D, H, non-S
Duke Upper	33.9879.09	*Acer rubrum*	23 (.89)	19 (.82)	14 (.56)	[a]	[a]	.04	.04	.06	MI	PK	PK	I	D, non-S
		Pinus taeda	16 (.84)	15 (.85)	11 (.36)	[a]	[a]	.13	.12	.12	MI	MI	MI	NC	D, non-S
		Quercus alba	19 (.80)	22 (.71)	21 (.58)	ns	ns	.1	.1	.14	ST	PK	PK	I	D
Parker Tract	33.05 76.91	*Pinus taeda*	.94 (.27)	1.1 (.42)	.91 (.45)	ns	ns	.08	.1	.09	PK	PK	PK	1	D
Jones Center	35.81 76.67	*Pinus palustris*	1.4 (.24)	1 (.35)	5 (.27)	[a]	[a]	.09	.22	.21	PK	PK	ST	NC	D, H, non-S; STORAGE
Crossett	31.22 84.48	*Pinus taeda*	1.3 (.26)	1.7 (.49)	1.3 (.34)	ns	ns	.25	.31	.34	PK	PK	ST	I	D; STORAGE

The slope parameter m represents the change in g_c as a function of $D^{-1/2}$ (i.e. Eqn. 8). The number in parentheses shows the coefficient of determination (i.e. R^2) of that regression. Nocturnal E_{SF} is that observed from 0 to 700 h and 1900 to 2300 h. NS, not significant; MI, E_{SF} is monotonically increasing with vapor pressure deficit (D); PK, E_{SF} peaks at some intermediate value of D; ST, E_{SF} is stationary for much of the day; NC, no visible change in the hysteresis between $g_{c,SF}$ and D at hourly timescales; I, hysteresis between $g_{c,SF}$ and D at hourly timescale increases for drier conditions; D, hysteresis between $g_{c,SF}$ and D at hourly timescale decreases for drier conditions; D, demand limitation; H, hydraulic limitation; non-S, non-stomatal limitation; STORAGE, a potential reliance on stored water.
[a]Which site species were associated with significantly different m between dry and wet conditions and int and wet conditions ($p < 0.05$, Student's t-test).

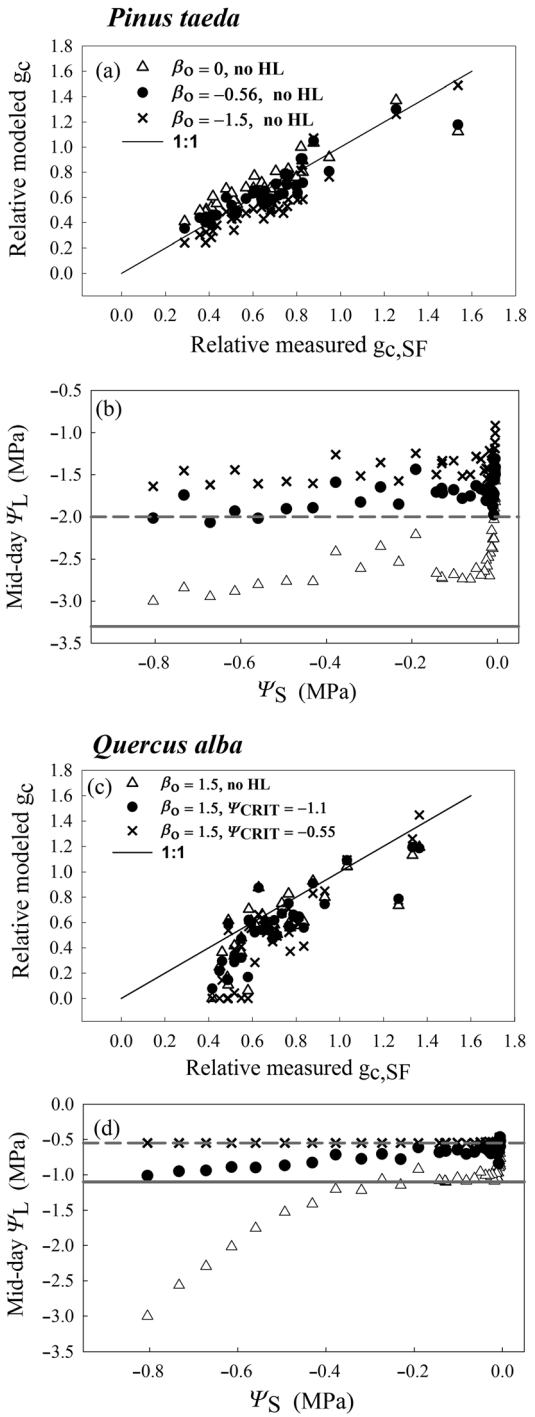

Figure 6. The top row shows a comparison of measured stomatal conductance inferred from sap flow observations ($g_{c,SF}$) and modelled stomatal conductance (g_c) for two species growing the Duke Forest. The model was driven with species-specific parameterizations for the relationship between K and Ψ_L and species-specific parameterizations for μ_{WW}. The sensitivity of μ to Ψ_L (i.e. β_o) and Ψ_{CRIT} determining the hydraulic limitation were varied as indicated in the legend. Data represent the daily averaged midday (1200–1500) stomatal conductance after normalizing by the value of $g_{c,sf}$ and g_c during well-watered conditions. The bottom rows show the simulated daily averaged midday Ψ_L as a function of daily averaged soil water potential (Ψ_S). The xylem air entry point (Ψ_e) and the leaf water potential associated with a 50% loss in K (Ψ_{50}) are also shown for reference as dashed lines.

and hydraulic architecture. Nonetheless, the qualitative nature of the relationships between gas exchange variables and D should be preserved regardless of the numerical values of the parameters.

Despite these limitations, this study presents an approach for explicitly linking optimality constraints, hydraulic constraints and non-stomatal considerations in a unified model framework. The coherent mapping of the model predictions to the empirical observations described in this study is encouraging and can inform and motivate ongoing efforts to explore how these different mechanisms jointly or independently regulate leaf-level gas exchange during drought. Such efforts are necessary given the relatively large degree of uncertainty associated with model formulations for g_c (Dietze *et al.* 2014) and the growing need for forest management activities that mitigate the deleterious effects of drought at species and ecosystem scales (Ford *et al.* 2011; Grant *et al.* 2013).

ACKNOWLEDGMENTS

We thank a number of individuals who assisted with data collection and analysis, including Rick Stagg, James Guldin, Mike Gavazzi, Steve McNulty, Jim Clark, David Bell, Becky Roper, Lindsey Boring, Jason McGee and in particular Barry Clinton, Daniel McInnis and Chris Sobek. We thank Stefano Manzoni and Rick Meinzer for providing valuable comments on earlier versions of the manuscript. This study was supported by the US Department of Agriculture Forest Service, Southern Research Station. The authors declare that they have no conflict of interest, financial or otherwise, that might be perceived as influencing their objectivity with respect to this work.

REFERENCES

Berninger F. & Hari P. (1993) Optimal regulation of gas exchange—evidence from field data. *Annals of Botany* **71**, 135–140.

Buckley T.N. (2005) The control of stomata by water balance. *New Phytologist* **168**, 275–291.

Buckley T.N. & Schymanski S.J. (2014) Stomatal optimisation in relation to atmospheric CO_2. *New Phytologist* **201**, 372–377.

Choat, B., Jansen, S., Brodribb, T.J., Cochard, H., Delzon, S., Bhaskar, R., … Zanne A.E. (2012) Global convergence in the vulnerability of forests to drought. *Nature* **491**, 752–755.

Comstock J. & Mencuccini M. (1998) Control of stomatal conductance by leaf water potential in *Hymenoclea salsola* (T & G), a desert subshrub. *Plant, Cell and Environment* **21**, 1029–1038.

Cook B.I., Ault T.R. & Smerdon J.E. (2015) Unprecedented 21st century drought risk in the American Southwest and Central Plains. *Sciences Advances* **1**, e1400082, DOI: 10.1126/sciadv.1400082.

Cowan I.R. (1986) Economics of carbon fixation in higher plants. *On the Economy of Plant Form and Function* (ed Givnish T.J.), pp. 133–170. Cambridge University Press, Cambridge.

Cowan I.R. & Farquhar G.D. (1977) Stomatal function in relation to leaf metabolism and environment. *Symposia of the Society for Experimental Biology* **31**, 471–505.

Dietze, M.C., Serbin, S.P., Davidson, C., Desai, A.R., Feng, X.H., Kelly, R., … Wang D. (2014) A quantitative assessment of a terrestrial biosphere model's data needs across North American biomes. *Journal of Geophysical Research-Biogeosciences* **119**, 286–300.

Domec, J.-C., Schafer, K., Oren, R., Kim, H.-S., McCarthy, H.R. (2010) Variable conductivity and embolism in roots and branches of four contrasting tree species and their impacts on whole-plant hydraulic performance under future atmospheric CO_2 condition. *Tree Physiology* **30**, 1001–1015.

Duursma, R.A., Barton, C.V.M., Lin, Y.-S., Medlyn, B.E., Eamus, D., Tissue, D. T., … McMurtrie, R.E. (2014) The peaked response of transpiration rate to vapour pressure deficit in field conditions can be explained by the temperature optimum of photosynthesis. *Agricultural and Forest Meteorology* **189**, 2–10.

Ewers B.E., Gower S.T., Bond-Lamberty B. & Wang C.K. (2005) Effects of stand age and tree species on canopy transpiration and average stomatal conductance of boreal forests. *Plant, Cell and Environment* **28**, 660–678.

Farquhar G.D., Caemmerer S.V. & Berry J.A. (1980) A biochemical model of photosynthetic CO_2 assimilation in leaves of C-3 species. *Planta* **149**, 78–90.

Flexas J., Barbour M.M., Brendel O., Cabrer H.M., Carriqui M., Diaz-Espejo A., … Warren C.R. (2012) Mesophyll diffusion conductance to CO_2: An unappreciated central player in photosynthesis. *Plant Science* **193–194**, 70–84.

Flexas J. & Medrano H. (2002) Drought-inhibition of photosynthesis in C-3 plants: stomatal and non-stomatal limitations revisited. *Annals of Botany* **89**, 183–189.

Ford C.R., Goranson C.E., Mitchell R.J., Will R.E. & Teskey R.O. (2004) Diurnal and seasonal variability in the radial distribution of sap flow: predicting total stem flow in *Pinus taeda* trees. *Tree Physiology* **24**, 941–950.

Ford C.R., Goranson C.E., Mitchell R.J., Will R.E. & Teskey R.O. (2005) Modeling canopy transpiration using time series analysis: a case study illustrating the effect of soil moisture deficit on *Pinus taeda*. *Agricultural and Forest Meteorology* **130**, 163–175.

Ford C.R., Laseter S.H., Swank W.T. & Vose J.M. (2011) Can forest management be used to sustain water-based ecosystem services in the face of climate change? *Ecological Applications* **21**, 2049–2067.

Franks P.J., Cowan I.R. & Farquhar G.D. (1997) The apparent feedforward response of stomata to air vapour pressure deficit: information revealed by different experimental procedures with two rainforest trees. *Plant, Cell and Environment* **20**, 142–145.

Grant G.E., Tague C.L. & Allen C.D. (2013) Watering the forest for the trees: an emerging priority for managing water in forest landscapes. *Frontiers in Ecology and the Environment* **11**, 314–321.

Grassi G. & Magnani F. (2005) Stomatal, mesophyll conductance and biochemical limitations to photosynthesis as affected by drought and leaf ontogeny in ash and oak trees. *Plant, Cell and Environment* **28**, 834–849.

Grassi G., Ripullone F., Borghetti M., Raddi S. & Magnani F. (2009) Contribution of diffusional and non-diffusional limitations to midday depression of photosynthesis in Arbutus unedo L. *Trees-Structure and Function* **23**, 1149–1161.

Hacke U.G., Sperry J.S., Ewers B.E., Ellsworth D.S., Schafer K.V.R. & Oren R. (2000) Influence of soil porosity on water use in Pinus taeda. *Oecologia* **124**, 495–505.

Hari P., Maekelae A., Korpilahti E. & Holmberg M. (1986) Optimal control of gas exchange. *Tree Physiology* **2**, 169–175.

Huntington T.G. (2006) Evidence for intensification of the global water cycle: review and synthesis. *Journal of Hydrology* **319**, 83–95.

Jarvis P.G. (1976) Interpretation of variations in leaf water potential and stomatal conductance found in canopies in field. *Philosophical Transactions of the Royal Society of London Series B-Biological Sciences* **273**, 593–610.

Johnson D.M., McCulloh K.A., Woodruff D.R. & Meinzer F.C. (2012) Hydraulic safety margins and embolism reversal in stems and leaves: why are conifers and angiosperms so different? *Plant Science* **195**, 48–53.

Kattge, J., Diaz, S., Lavorel, S., Prentice, C., Leadley, P., Bonisch, G., … Wirth, C. (2011) TRY—a global database of plant traits. *Global Change Biology* **17**, 2905–2935.

Katul G., Manzoni S., Palmroth S. & Oren R. (2010) A stomatal optimization theory to describe the effects of atmospheric CO2 on leaf photosynthesis and transpiration. *Annals of Botany* **105**, 431–442.

Katul G.G., Ellsworth D.S. & Lai C.T. (2000) Modelling assimilation and intercellular CO_2 from measured conductance: a synthesis of approaches. *Plant, Cell and Environment* **23**, 1313–1328.

Katul G.G., Palmroth S. & Oren R. (2009) Leaf stomatal responses to vapour pressure deficit under current and CO2-enriched atmosphere explained by the economics of gas exchange. *Plant, Cell and Environment* **32**, 968–979.

Kim D., Oren R., Oishi A.C., Hsieh C.-I., Phillips N., Novick K.A. & Stoy P.C. (2014) Sensitivity of stand transpiration to wind velocity in a mixed broadleaved deciduous forest. *Agricultural and Forest Meteorology* **187**, 62–71.

Klein T., Shpringer I., Fikler B., Elbaz G., Cohen S. & Yakir D. (2013) Relationships between stomatal regulation, water-use, and water-use efficiency of two coexisting key Mediterranean tree species. *Forest Ecology and Management* **302**, 34–42.

Lawlor D.W. & Tezara W. (2009) Causes of decreased photosynthetic rate and metabolic capacity in water-deficient leaf cells: a critical evaluation of mechanisms and integration of processes. *Annals of Botany* **103**, 561–579.

Lens F., Sperry J.S., Christman M.A., Choat B., Rabaey D. & Jansen S. (2011) Testing hypotheses that link wood anatomy to cavitation resistance and hyraulic conductivity in the genus *Acer*. *New Phytologist* **190**, 709–723.

Leuning R., Kelliher F.M., Depury D.G.G. & Schulze E.D. (1995) Leaf nitrogen, photosynthesis, conductance and transpiration—scaling from leaves to canopies. *Plant, Cell and Environment* **18**, 1183–1200.

Limousin J.M., Misson L., Lavoir A.V., Martin N.K. & Rambal S. (2010) Do photosynthetic limitations of evergreen *Quercus ilex* leaves change with long-term increased drought severity? *Plant Cell and Environment* **33**, 863–875.

Loreto F., Harley P.C., Di Marco G. & Sharkey T.D. (1992) Estimation of mesophyll conductance to CO_2 flux by three different methods. *Plant Physiology* **98**, 1437–1443.

Maherali H., Moura C.F., Caldeira M.C., Willson C.J. & Jackson R.B. (2006) Functional coordination between leaf gas exchange and vulnerability to xylem cavitation in temperate forest trees. *Plant, Cell and Environment* **29**, 571–583.

Makela A., Berninger F. & Hari P. (1996) Optimal control of gas exchange during drought: theoretical analysis. *Annals of Botany* **77**, 461–467.

Manzoni S., Vico G., Katul G., Fay P.A., Polley W., Palmroth S. & Porporato A. (2011) Optimizing stomatal conductance for maximum carbon gain under water stress: a meta-analysis across plant functional types and climates. *Functional Ecology* **25**, 456–467.

Manzoni S., Vico G., Palmroth S., Porporato A. & Katul G. (2013) Optimization of stomatal conductance for maximum carbon gain under dynamic soil moisture. *Advances in Water Resources* **62**, 90–105.

Martinez-Vilalta J., Poyatos R., Aguade D., Retana J. & Mencuccini M. (2014) A new look at water transport regulation in plants. *New Phytologist* **204**, 105–115.

Matheny A.M., Bohrer G., Vogel C.S., Morin T.H., He L., Frasson R.P.M., … Curtis P.S. (2014) Species-specific transpiration responses to intermediate disturbance in a northern hardwood forest. *Journal of Geophysical Research-Biogeosciences* **119**, 2292–2311.

McDowell, N., Pockman, W.T., Allen, C.D., Breshears, D.D., Cobb, N., Kolb, T., … Yepez E.A. (2008) Mechanisms of plant survival and mortality during drought: why do some plants survive while others succumb to drought? *New Phytologist* **178**, 719–739.

Medlyn, B.E., Duursma, R.A., Eamus, D., Ellsworth, D.S., Prentice, I.C., Barton, C.V.M., … Wingate L. (2011) Reconciling the optimal and empirical approaches to modelling stomatal conductance. *Global Change Biology* **17**, 2134–2144.

Meinzer F.C., James S.A. & Guillermo G. (2004) Dynamics of transpiration, sap flow and use of stored water in tropical forest tree species. *Tree Physiology* **24**, 901–909.

Meinzer F.C., Johnson D.M., Lachenbruch B., McCulloh K.A. & Woodruff D.R. (2009) Xylem hydraulic safety margins in woody plants: coordination of stomatal control of xylem tension with hydraulic capacitance. *Functional Ecology* **23**, 922–930.

Meinzer F.C., Woodruff D.R., Marias D.E., McColluh K.A. & Savanto S. (2014) Dynamics of leaf water relations components in co-occurring iso- and anisohydric conifer species. *Plant, Cell and Environment* **37**, 2577–2586.

Niinemets Ü., Diaz-Espejo A., Flexas J., Galmés J. & Warren C.R. (2009) Importance of mesophyll diffusion conductance in estimation of plant photosynthesis in the field. *Journal of Experimental Botany* **60**, 2271–2282.

Niinemets Ü., Cescatti A., Rodeghiero M. & Tosens T. (2005) Leaf internal diffusion conductance limits photosynthesis more strongly in older leaves of Mediterranan evergreen broad-leaved species. *Plant, Cell and Environment* **28**, 1552–1566.

Novick K.A., Oishi A.C., Ward E.J., Siqueira M.B.S., Juang J.Y. & Stoy P.C. (2014) On the difference in the net ecosystem exchange of CO_2 between deciduous and evergreen forests in the southeastern U.S. *Global Change Biology* **21**, 827–842.

O'Grady A.P., Eamus D. & Hutley L.B. (1999) Transpiration increases during the dry season: patterns of tree water use in eucalypt open-forests of northern Australia. *Tree Physiology* **19**, 591–597.

Oren R., Sperry J.S., Katul G.G., Pataki D.E., Ewers B.E., Phillips N. & Schafer K.V.R. (1999) Survey and synthesis of intra- and interspecific variation in stomatal sensitivity to vapour pressure deficit. *Plant, Cell and Environment* **22**, 1515–1526.

Palmroth S., Katul G.G., Maier C.A., Ward E., Manzoni S. & Vico G. (2013) On the complementary relationship between marginal nitrogen and water-use efficiencies among *Pinus taeda* leaves grown under ambient and CO_2-enriched environments. *Annals of Botany* **111**, 467–477.

Phillips N.G., Ryan M.G., Bond B.J., McDowell N.G., Hinckley T.M. & Cermak J. (2003) Reliance on stored water increases with tree size in three species in the Pacific Northwest. *Tree Physiology* **23**, 237–245.

Plaut J.A., Yepez E.A., Hill J., Pangle R., Sperry J.S., Pockman W.T. & McDowell N.G. (2012) Hydraulic limits preceding mortality in a pinon-juniper woodland under experimental drought. *Plant Cell & Environment* **35**, 1601–1617.

Roman D.T., Novick K.A., Brzostek E.R., Dragoni D., Rahman A.F. & Phillipps, R. (2015) The role of isohydric and anisohydric species in determining ecosystem scale response to severe drought. *Oecologia* **173**, 641–654.

Sade N., Gebremedhin A. & Moshelion M. (2012) Risk-taking plants: anisohydric behavior as a stress-resistance trait. *Plant Signaling & Behavior* **7**, 767–770.

Scholz F.G., Phillips N.G., Bucci S.J., Meinzer F.C. & Goldstein, G. (2011) Hydraulic capacitance: biophysics and functional significance of internal water sources in relation to tree size. In: Meinzer, F.C., Lachenbruch, B., Dawson, T. E. (eds). *Size- and age-related changes in tree structure and function*. Springer, Dordrecht, pp 341–361.

Schulze E.D., Buschbom U., Evenari M., Lange O.L. & Kappen L. (1972) Stomatal responses to changes in humidity in plants growing in desert. *Planta* **108** 259-&.

Sperry J.S. (2000) Hydraulic constraints on plant gas exchange. *Agricultural and Forest Meteorology* **104**, 13–23.

Stoy P.C., Katul G.G., Siqueira M.B.S., Juang J.Y., Novick K.A., Uebelherr J.M. & Oren R. (2006) An evaluation of models for partitioning eddy covariance-measured net ecosystem exchange into photosynthesis and respiration. *Agricultural and Forest Meteorology* **141**, 2–18.

Tezara W., Mitchell V.J., Driscoll S.D. & Lawlor D.W. (1999) Water stress inhibits plant photosynthesis by decreasing coupling factor and ATP. *Nature* **401**, 914–917.

Tyree M.T. & Sperry J.S. (1988) Do woody plants operate near the point of catastrophic xylem dysfunction caused by dynamic water-stress—answers from a model. *Plant Physiology* **88**, 574–580.

Unsworth, M.H., Phillips, N., Link, T., Bond, B.J., Falk, M., Harmon, M.E., … U, K.T.P. (2004) Components and controls of water flux in an Old-growth Douglas-fir—Western Hemlock ecosystem. *Ecosystems* **7**, 468–481.

Vico G., Manzoni S., Palmroth S. & Katul G. (2011) Effects of stomatal delays on the economics of leaf gas exchange under intermittent light regimes. *New Phytologist* **192**, 640–652.

Vico G. & Porporato A. (2008) Modelling C-3 and C-4 photosynthesis under water-stressed conditions. *Plant and Soil* **313**, 187–203.

Ward E.J., Bell D.M., Clark J.S. & Oren R. (2013) Hydraulic time constants for transpiration of loblolly pine at a free-air carbon dioxide enrichment site. *Tree Physiology* **33**, 123–134.

Wilhite D.A. & Glantz M.H. (1985) Understanding the drought phenomenon: the role of definitions. *Water International* **10**, 111–120.

Wullschleger S.D., Meinzer F.C. & Vertessy R.A. (1998) A review of whole-plant water use studies in trees. *Tree Physiology* **18**, 499–512.

Zhang Q., Manzoni S., Katul G., Porporato A. & Yang D. (2014) The hysteretic evapotranspiration—vapor pressure deficit relation. *Journal of Geophysical Research-Biogeosciences* **119**, 125–140.

Zhou S., Medlyn B., Sabate S., Sperlich D. & Prentice I. C. (2014) Short-term water stress impacts on stomatal, mesophyll and biochemical limitations to photosynthesis differ consistently among tree species from contrasting climates. *Tree Physiology* **34**, 1035–1046.

Zweifel R., Item H. & Hasler R. (2001) Link between diurnal stem radius changes and tree water relations. *Tree Physiology* **21**, 869–877.

Received 26 October 2014; accepted for publication 14 September 2015

SUPPORTING INFORMATION

Additional Supporting Information may be found in the online version of this article at the publisher's website:

Figure S1. Representative dynamics of the assumed stored water flux (*Fs*).
Figure S2. Meteorological variables recorded over the Duke Forest (Durham, NC, USA) in late summer, 2005 used to drive the model scenarios for a prototypical dry-down event. Ta is air temperature, Q is photosynthetically active radiation, and D is vapor pressure deficit.
Figure S3. Sap flux observations from the Duke Forest Sites:
Table S1. Model parameters, their definition, units, and assumed value. The final column shows which of the model scenarios (described in Table 1) for which the parameter applies.
Table S2. The RAFES study sites.